Composites Science and Technology 91 (2014) 38–44

Contents lists available at ScienceDirect

Composites Science and Technology

journal homepage: www.elsevier.com/locate/compscitech

A numerical study on carbon nanotube–hybridized carbon fibre pullout

Yuanyuan Jia [a], Zuorong Chen [b], Wenyi Yan [a,*]

[a] Department of Mechanical and Aerospace Engineering, Monash University, Wellington Road, Clayton, Victoria 3800, Australia
[b] CSIRO Earth Science & Resource Engineering, Clayton North, Victoria 3169, Australia

ARTICLE INFO

Article history:
Received 19 July 2013
Received in revised form 12 November 2013
Accepted 23 November 2013
Available online 8 December 2013

Keywords:
A. Hybrid composites
A. Nano composite
B. Interfacial strength
C. Finite element analysis (FEA)
Carbon nanotube/carbon fibre

ABSTRACT

Carbon nanotube (CNT)–hybridized carbon fibre (CF) composite is a new generation composite, where CNTs grow radially on carbon fibres to form a hybrid reinforcing phase. To evaluate the bridging effect of this new reinforcing phase, a numerical method is proposed to theoretically investigate the pullout of a hybrid fibre. There are two finite element models developed in this method, which are applied to simulate a single CNT pullout from the matrix at microscale and the pullout of the hybrid fibre at macroscale. The bridging effect of the CNTs during the hybrid fibre pullout is simulated by spring elements in the macroscale finite element model, where the properties of spring elements are obtained from the microscale finite element simulation. The numerical results indicate that the apparent interfacial shear strength of the hybrid fibre and the specific pullout energy can be significantly increased due to the additional bonding of the CNT–matrix interface. A parametric study indicates that the bridging effect of the hybrid fibre can be further enhanced by improving the interfacial bonding between CNT and matrix and increasing the size or length of CNTs. This study provides a new numerical method to simulate the multiscale CNT/CF hybrid fibre pullout.

1. Introduction

Carbon nanotubes (CNTs) are the finest and strongest fibres with a nanoscale diameter and length ranging from micro- to millimetres [1]. CNTs are widely used in many areas, such as electronics, nano-electro-mechanical devices and medical applications. In the past few years, studies have been carried out to better understand the mechanical performance of CNT-reinforced composites. It showed that a small quantity of nanotubes added to a polymer matrix can increase the stiffness and strength of the composite [2,3]. For example, dispersing 1 wt% of CNTs to a matrix material results in up to 42% increase in the stiffness of the composite [2]. However, directly dispersing CNTs to the resin has difficulty in controlling the alignment and orientation of the CNTs and, therefore, there will be difficulties in controlling the quality of the produced CNT-based composites.

A recent development of CNT composites is through chemical vapour deposition (CVD) to grow CNTs radially on micro-fibres, such as carbon fibres, and to use these hybrid fibres to develop superior 3D composites, carbon nanotube (CNT)/carbon fibre (CF) hybrid composites [4]. CNT/CF hybrid composites combine the advantages of both the carbon fibres and the carbon nanotubes. Because traditional fibres only provide in-plane reinforcement, delamination can easily occur since there is no reinforcement in the direction of the z coordinate (through-thickness direction) to resist crack initiation and propagation. Since the CNTs align in multi-directions in the matrix, they can provide reinforcement to the matrix in different directions as a 3D reinforcement. Due to the extremely high tensile strength, stiffness and the increased interfacial area, it is expected that the fracture toughness of the new composites with the hybrid 3D reinforcement will be increased substantially.

The performance of a composite critically depends on the interfacial properties between the reinforcing phase and the matrix phase. Interfacial shear strength is a key parameter to determine the efficiency of load transfer from the polymer matrix to the fibres. Recent results have shown the improvement of the interfacial strength between the fibres and matrix by growing CNTs on the surfaces of carbon fibres [4–8]. A single fibre pullout test is one of the widely used techniques to quantify the interfacial strength. A few studies have been carried out to understand the mechanical performance of CNTs reinforced composites using the single fibre pullout test [9–11].

In comparison to experimental research, theoretical and numerical analysis can provide additional insight into the reinforcing effect of CNTs-based nanocomposites, which can assist the further development and design optimisation of composites. Several numerical studies have been carried out on the CNT pullout [12–15], but no numerical study on CNT/CF hybrid fibre pullout has been reported. It is due to the complexity of pullout process of the hybrid fibre and the two different scales of the CNTs and

* Corresponding author. Tel.: +61 3 9902 0113; fax: +61 3 9905 1825.
E-mail address: wenyi.yan@monash.edu (W. Yan).

0266-3538/$ - see front matter © 2013 Elsevier Ltd. All rights reserved.
http://dx.doi.org/10.1016/j.compscitech.2013.11.020

the fibre–matrix. Kulkarni et al. [16] and Nie et al. [17] developed two similar multiscale models to evaluate the effect of interfacial strength on the elastic modulus of hybrid fibre reinforced polymer composites. They firstly modelled a nanocomposite formed by a single CNT–matrix and numerically predicted the overall mechanical properties of the nanocomposite. The second step is to consider the nanocomposite as an equivalent matrix and use it to form a single carbon fibre nanoreinforced laminated composite. No CNT/CF hybrid fibre pullout was studied in these two papers.

The purpose of this paper is to develop a numerical method to simulate the pullout of a single CNT/CF hybrid fibre. The interfacial bonding between the hybrid fibre and the matrix, and the bridging effects of the hybrid fibre on the composite are able to be theoretically examined by using this method. The bonding and debonding behaviours between the carbon fibre–matrix interface and between the CNT–matrix interface are described by cohesive laws. In addition, the effect of relevant parameters of CNTs on the hybrid fibre pullout behaviour is discussed.

2. Numerical method for hybrid fibre pullout

CNTs can be radially grown on the surface of carbon fibres and then embedded in an epoxy matrix to produce CNT/CF hybrid fibre reinforced composite, as shown in Fig. 1(a) [11]. During the hybrid fibre pullout, there are two types of interfaces, carbon fibre–matrix interface and CNT–matrix interface. As the pullout force is applied to the carbon fibre, both shear and tensile load can be transferred to the CNTs. The stresses in the CNTs will be transferred to the matrix through CNT–matrix interface. As the pullout force increases, cracks initiate and propagate along both interfaces of carbon fibre–matrix and CNT–matrix, which leads to the debonding of the carbon fibre–matrix interface and CNT–matrix interface.

To numerically simulate the complicated hybrid fibre pullout, a few assumptions are made to simplify the problem:

(1) It is assumed that the CNTs are uniformly grown on the carbon fibre and they are ideally aligned in the radial direction. As shown in Fig. 1(a), CNTs are densely distributed on the fibre, and therefore, the assumption of the uniform CNTs distribution is acceptable. Due to the large amount of CNTs, the effects of the curvature and the direction misalignment of individual CNTs are almost impossible to simulate and therefore, these effects are neglected in this theoretical study.
(2) All the CNTs are assumed to have identical geometry (including the radius and the length) and mechanical property. The bonding and debonding behaviour of the interfaces between individual CNTs and the matrix is also assumed to be the same. Based on this assumption, the bridging effects of all the CNTs are identical and only a single CNT pullout study is needed.
(3) Possible matrix damage during the hybrid fibre pullout is neglected in this numerical study.

Based on these assumptions, an idealized hybrid fibre pullout problem is illustrated in Fig. 1(b).

During the single CNT/CF hybrid fibre pullout, there are two physical phenomena, which occur at two different scales: CNT pullout at microscale and carbon fibre pullout at macroscale. To overcome the difficulties in the simulation of the multiscale problem, a numerical method is proposed to deal with the two pullout processes explicitly but in two separate finite element models. A finite element model at microscale is applied to simulate a single CNT pullout from the matrix and another finite element model at macroscopic scale is applied to simulate the pullout of the hybrid fibre. The bridging effect of the CNTs during the hybrid fibre pullout is simulated by using equivalent spring elements in the macroscale hybrid fibre pullout model, where the spring elements' property is obtained from the microscale CNT pullout simulation.

2.1. Finite element model for CNT pullout at microscale

Some numerical methods have been developed to study the CNT–matrix interface by using the molecular dynamic (MD) method and the finite element method. Examples on the study of using the MD method can be found in [12,15,18,19], where the bonded and nonbonded potentials are represented in terms of the force constants and the change in distance among the atomic bonds. However the length of the CNT in the MD models is limited to the range of 4–10 nm because of the intensive computational requirements in the MD simulation [13,15,16,20]. Due to this limitation, applying MD method to study the pullout of CNTs with the length in several micrometres is unachievable. On the other hand, CNTs have been described as a continuum solid beam or shell subjected to tension, bending, or torsional forces by applying continuum mechanics [14,20,21]. In this way, the nanoscale dimension in the thickness direction of the CNTs is not explicitly involved in the models. The nano- and the microscales problem becomes a single microscale problem. In the current study, the continuum mechanics is applied to treat CNTs as membranes.

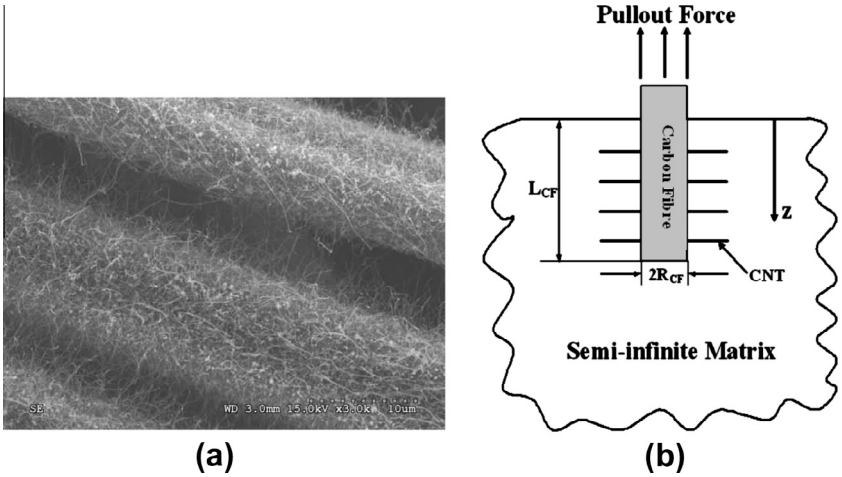

Fig. 1. (a) SEM image of hybrid fibres with CNTs [11]; and (b) a schematic diagram of the idealized CNT/CF hybrid fibre pullout problem.

The finite element method is used to simulate the single CNT pullout at microscale, which is described below.

In the single CNT pullout, a two-dimensional axisymmetric model at microscale was developed using a single cylindrical CNT embedded in a semi-infinite matrix. A pullout displacement was applied on the top of the CNT in the axial direction, as shown in Fig. 2(a). In this study, a 24 nm diameter carbon nanotube is embedded in an epoxy matrix with the embedded length L_{CNT} = 2.6 μm, which is consistent with the experiment by Cooper et al. [22]. The Young's modulus of CNT was taken as E_{CNT} = 1.1 TPa with the wall thickness = 0.34 nm, and epoxy matrix with E_m = 3.4 GPa was used in this study. Membrane elements (MAX1) were used in commercial finite element package Abaqus to represent the cylindrical CNT. Membrane elements can be used to represent a thin surface in space which offers strength in the plane of the element without bending stiffness [23]. In addition, the axisymmetric cohesive elements (COHAX4) were used to define the cohesive zone between the interface of the CNT and the matrix.

2.1.1. Cohesive law

Cohesive zone modelling is a commonly used technique to investigate the failure governed by crack or debonding propagation [24–26]. Namilae and Chandra [14] used the results of CNT pullout from MD simulation to evaluate cohesive zone model parameters. Their traction-displacement plots were obtained by averaging the pullout load with the applied displacements and dividing by the corresponding area. Unfortunately, these traction-displacement plots were unable to show the complete failure of the interface. Therefore the traction-displacement plots used in their cohesive zone were redefined by extrapolating curves to complete failure. Liu et al. [13] also proposed a cohesive interface model based on MD simulation results. However their MD model needs to be further verified against experimental results.

In the current study, a cohesive zone model was adopted from Tvergaard [27] and Chaboche et al. [28]. Their interface debonding model has been used extensively and it is capable of capturing the progressive decohesion of the interface. The interfacial debonding during a CNT pullout is a pure mode II fracture problem. Therefore the mode II cohesive law [28] can be simplified as

$$T_t = \left(\frac{27u_t^3}{4\delta_t^3} - \frac{27u_t^2}{2\delta_t^2} + \frac{27u_t}{4\delta_t}\right)\tau_{\max(CNT)} \quad (1)$$

where u_t is the tangential separation, δ_t is the complete tangential separation, and $\tau_{\max(CNT)}$ is the interfacial crack initiation stress under shear loading condition as shown in Fig. 2(b). Correlating to energy-based fracture mechanics, the fracture energy release rate G_{IIc} is the area under the traction–separation curve.

2.2. Finite element model for CNT/CF hybrid fibre pullout at macroscale

The physical problem of the CNT/CF hybrid fibre pullout was treated as a cylindrical carbon fibre embedded in a semi-infinite matrix and attached with the CNTs (Fig. 1(b)). The radius of the fibre is denoted as R_{CF} and L_{CF} is the total embedded fibre length. As the model developed in carbon fibre pullout [29], a pullout displacement was applied uniformly on the top surface of the fibre in the axial direction. It is assumed that the normal stress along the carbon fibre does not exceed its material ultimate strength, so the carbon fibre will not break before it is pulled out. The plastic behaviour in the fibre will not be considered in this paper.

Due to the symmetry of this problem, a two-dimensional axisymmetric model was constructed. The radius and depth of the matrix in the model are much larger than the dimensions of the fibre so as to treat the matrix as a semi-infinite body. The model contains a total of 5149 four-node quadrilateral elements. A very fine mesh with the smallest elements (CAX4) of 1 μm × 1 μm were used in the area around the interface as shown in Fig. 3(b). A small number of four-node, axisymmetric cohesive elements (COHAX4) were used to define the cohesive zone. Nonlinear spring elements (SPRING1) were used to model the bridging effect of CNTs in the CNT/CF hybrid fibre pullout, as shown in Fig. 3(a). In the pullout simulation, the spring elements were elongated and the spring forces resisted the pullout of the carbon fibre [30,31]. The nonlinear spring elements' properties were obtained from the pullout curve from the microscale CNT pullout simulation. Since the spring elements are used to simulate the force of CNTs applied on the carbon fibre, the debonding of CNT–matrix interface will not be explicitly simulated in the hybrid fibre pullout model. Therefore the debonding only occurs between the carbon fibre and matrix interface, which is assumed to initiate at the carbon fibre–matrix interface and propagate longitudinally along the carbon fibre.

Referring to Fig. 1(b), the CNTs are aligned in the matrix at an inclination angle of 90° with respect to pullout direction. Therefore, the vertical resistance force applied on the fibre $F_{CNT(90°)}$ is transferred from the horizontal force $F_{CNT(0°)}$, the direct CNT pullout force along the CNT's axial direction. This force transition is estimated through a frictional pulley model. In this case, the CNT is treated as a flexible string passing over a frictional pulley, and therefore a snubbing friction model can be derived to relate the pullout force to the fibre inclination angle [32],

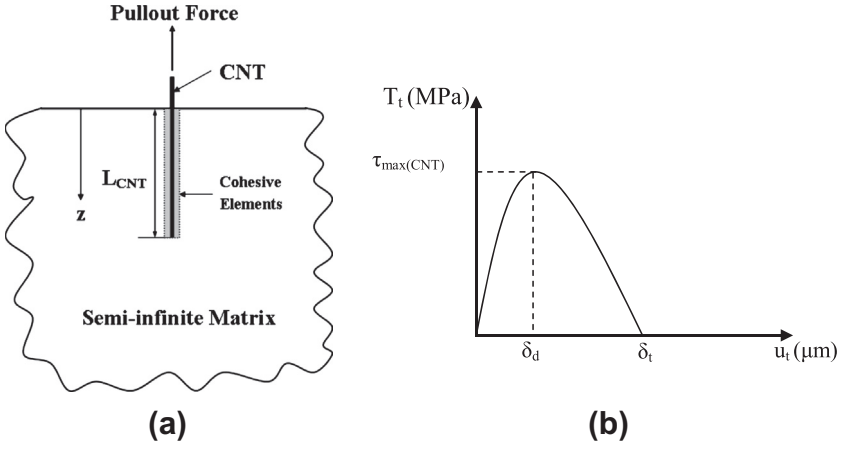

Fig. 2. (a) A schematic diagram of a single CNT pullout model; and (b) cohesive law used for the single CNT pullout model.

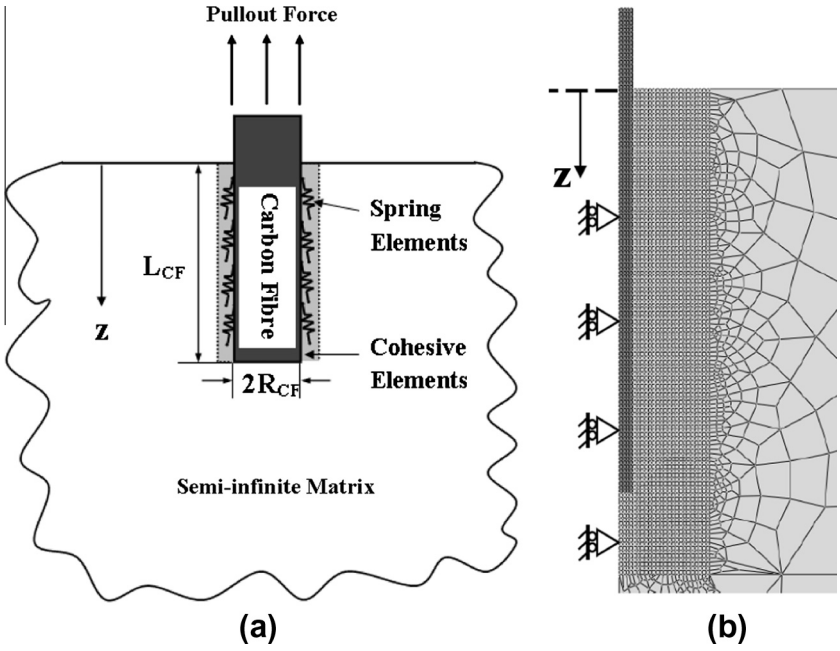

Fig. 3. (a) A schematic diagram of the CNT/CF hybrid fibre pullout model using spring elements to simulate the resistance of the CNTs; and (b) axisymmetric finite element model for a single CNT/CF hybrid fibre pullout with a fine mesh around the interface.

$$F_{CNT(90^\circ)} = F_{CNT(0^\circ)} e^{f\Phi} \quad (2)$$

where $F_{CNT(0^\circ)}$ is the CNT pullout force from the microscale finite element simulation, $F_{CNT(90^\circ)}$ is the pullout force of inclined CNT with the pullout direction $\Phi = 90^\circ$, and f is the snubbing friction coefficient [32]. In the hybrid fibre pullout, the pullout force $F_{CNT(90^\circ)}$ from Eq. (2) was applied to define the nonlinear properties of the spring elements. Since the CNTs are highly flexible, the snubbing friction coefficient can be assumed as a small value $f = 0.1$ [33]. Some studies have shown that this simple frictional pulley model (Eq. (2)) is able to represent the effect of fibre pullout angle on the pullout load [32,34,35].

2.2.1. Simulation of CNT effect in macroscale finite element model

In this study, the length and number of CNTs were estimated based on the experimental results obtained by Zhang et al. [36]. The length of CNTs (L_{CNT}) grown on the carbon fibre was estimated at 6.5 μm. The number of CNTs grown on the carbon fibre was calculated based on the CNT population density estimated from the experiment. Based on the assumption of uniformly distributed CNTs, the number of CNTs grown on the carbon fibre per unit length can be calculated as 1760 tubes/μm. It was also assumed that there were 100 layers of CNTs, which means there were 100 spring elements in the macroscale finite element model uniformly distributed along the carbon fibre–matrix interface ($L_{CF} = 100$ μm with element size 1 μm × 1 μm). Therefore, the total number of CNTs distributed on each layer was estimated as 1760 tubes, which was represented by a single spring element. It is worth noting that CNT breaking or detaching from the carbon fibre, which may occur in practice, can be considered in this model by cutting of the nonlinear force–displacement curve of the spring elements. Due to length limitation, it was not presented in the paper.

3. Results and discussion

3.1. Single CNT pullout simulation

A comparison study between a finite element simulation at microscale and an experimental single CNT pullout test was carried out. Fig. 4 shows the simulated single CNT pullout curve. The numerical results were compared with the experimental results from Cooper et al. [22]. In this study, the maximum pullout force $F_{\max(CNT)}$ and the total CNT pullout energy W_{CNT} were found to be 6.845 μN and 1.63×10^{-12} J, respectively, which agree well with the experimental results ($F_{\max(CNT)} = 6.8 \pm 1.7$ μN and $W_{CNT} = 1.6 \times 10^{-12}$ J) with these fitted parameters $\tau_{\max(CNT)} = 36$ MPa, $\delta_{d(CNT)} = 140$ nm, $\delta_{t(CNT)} = 410$ nm. The pullout force–displacement curve is used to define the nonlinear properties of the spring elements in the hybrid fibre pullout simulation.

3.2. CNT/CF hybrid fibre pullout

3.2.1. CNT/CF hybrid fibre pullout force

The debonding force of hybrid fibre ($F_{\max(H)}$), is one of the most important parameters recorded from a pullout test, which is used to calculate the average interfacial strength. Fig. 5 shows the case of CNTs completely pulled out with the carbon fibre, compared with a single carbon fibre pullout. It can be seen that the pullout force of the hybrid fibre increases rapidly due to the bonding

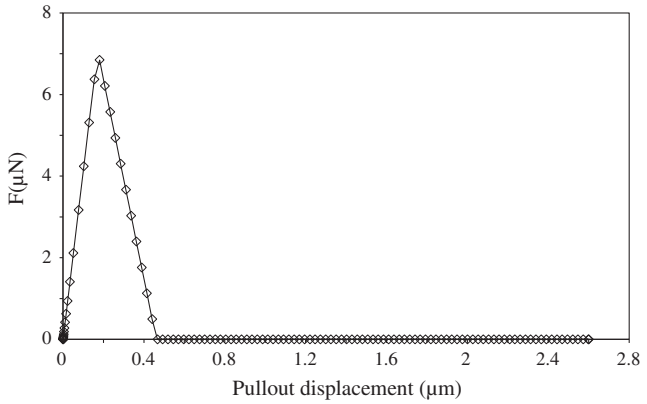

Fig. 4. Single CNT pullout curve from the microscale finite element simulation.

between CNTs and the matrix. It reaches the maximum debonding force when the pullout displacement approaches 3 μm. The force then drops quickly due to debonding in the CNT–matrix interfaces. After the CNT–matrix interfaces have completely debonded, the hybrid fibre pullout curve coincides with the carbon fibre pullout curve. Fig. 5 also shows that the magnitude of the debonding force for CNT/CF hybrid fibre ($F_{max(H)}$ = 0.39 N) is much higher than that for the carbon fibre pullout ($F_{max(CF)}$ = 0.1 N). The debonding force of the hybrid fibre has a significant increase of 290%. The increased pullout force was observed before the interfacial debonding occurred in carbon fibre. An et al. [9] performed an experiment of the CNT/CF hybrid fibre pullout and reported that the debonding force of hybrid fibre had a significant increase up to 120%. The difference may be due to the different number of CNTs and embedded length of carbon fibre used in this study.

3.2.2. Interfacial shear strength

The interfacial shear strength (IFSS) is traditionally used to evaluate the interfacial bonding. In this study, the apparent interfacial shear strength τ_{app} was calculated from the debonding force of hybrid fibre, $F_{max(H)}$, and interfacial area of carbon fibre–matrix using the following equation [37]

$$\tau_{app} = \frac{F_{max(H)}}{2\pi R_{CF} L_{CF}} \tag{3}$$

The apparent interfacial shear strength increased 290% (45.5 MPa to 177 MPa). This improvement is due to the increased bonding in the CNT–matrix interface. A significant improvement in the IFSS was also observed in the experimental studies [7,9,10,38,39]. This numerical study investigated an ideal case of CNTs grown on the carbon fibre. Practically, the performance of hybrid composites is significantly influenced by density or morphology of CNT grown on the fibre surface, such as tangled CNTs, partial coverage of aligned CNTs and "mohawk" aligned CNTs [40]. Consequently, this predicted IFSS increase is higher than those experimental results. Nevertheless, this study confirms that growing CNTs on the carbon fibre can enhance the adhesion between the reinforcing phase and the matrix, and thus improve the intralaminar fracture toughness of the composite. In addition, applying Eq. (2) and the peak CNT pullout force, the shear stress at the joint of the CNT and carbon fibre was estimated as 38 GPa, which is unusually large. Practically, the CNT will detach from the carbon fibre if the shear strength at the joint is lower than the shear stress, which have been observed in experiment [9]. On the other hand, the joint shear strength can be increased by using particular catalysts [41,42].

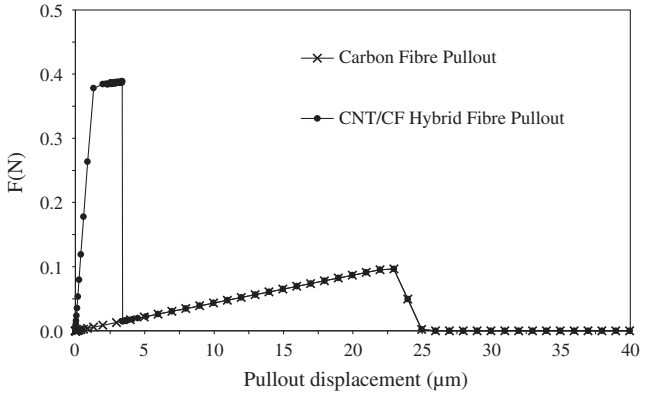

Fig. 5. Comparison between the numerical results of the single carbon fibre and the single CNT/CF hybrid fibre complete pullout curve.

3.2.3. Specific pullout energy

Specific pullout energy can be used to quantify the bridging effect of the CNTs during the hybrid fibre pullout. The specific pullout energy of hybrid fibre ω_H is defined as

$$\omega_H = \frac{W_H}{2\pi R_{CF} L_{CF}} \tag{4}$$

where W_H is the total hybrid fibre pullout energy, which is the total area under the pullout force–displacement curve. Fibre bridging appears behind a major crack tip in an intralaminar fracture, which enhances the fracture resistance of fibre reinforced composite. The magnitude of the specific pullout energy of CNT/CF hybrid fibre (ω_H = 1032 J/m^2) is much higher than the carbon fibre [29] (ω_{CF} = 565 J/m^2). The specific pullout energy of the CNT/CF hybrid fibre increases by 83%. This is due to the large resistance induced by the CNTs, which requires more energy to pull out the hybrid fibre. This significant improvement of toughness was observed in the experimental study by Garcia et al. [39], which reported a 150–300% increase of toughness. The difference in the number and geometry of CNTs between this study and the experiment can contribute to the difference in the increase of the toughness value.

3.3. Bridging effect of CNTs in CNT/CF hybrid fibre pullout

In a single CNT pullout, the interfacial bonding of CNT–matrix and the geometry of CNT are two main factors to influence the CNT pullout, and therefore the hybrid fibre pullout.

3.3.1. Effect of interfacial bonding between CNT and matrix

The interfacial bonding effect is dependent on two dominant parameters, $\tau_{max(CNT)}$ and $\delta_{t(CNT)}$, based on the cohesive law used in the single CNT pullout simulation (Eq. (1)). In this parametric study, $\tau_{max(CNT)}$ varies from 15 MPa to 45 MPa and $\delta_{t(CNT)}$ varies from 0.2 μm to 0.8 μm. Fig. 6 shows the relationship between the debonding force ($F_{max(H)}$) of CNT/CF hybrid fibre pullout and the interfacial crack initiation shear stress ($\tau_{max(CNT)}$) of the CNT–matrix interface. It clearly indicates that the debonding force of hybrid fibre increases almost linearly with the increase of interfacial crack initiation shear stress in all cases. The figure also indicates that the debonding force of the hybrid fibre pullout increases as the complete tangential separation $\delta_{t(CNT)}$ increases. This is due to the increased pullout force $F_{max(CNT)}$ from the single CNT pullout. In the single CNT pullout, the CNT pullout force $F_{max(CNT)}$ increases as the interfacial crack initiation shear stress ($\tau_{max(CNT)}$) or complete tangential separation $\delta_{t(CNT)}$ increases.

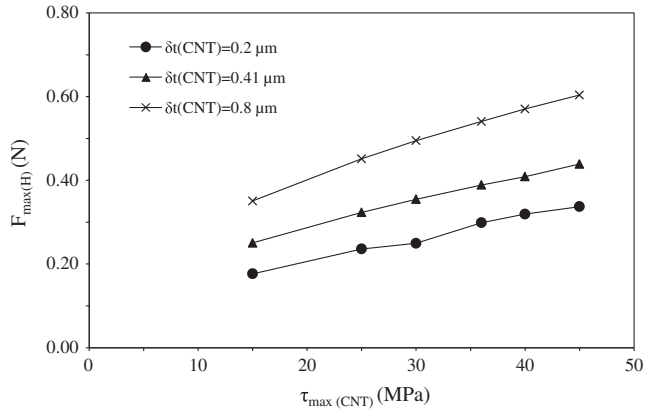

Fig. 6. Influence of interfacial crack initiation shear stress of CNT $\tau_{max(CNT)}$ on the debonding force with different values of CNT complete separation displacement $\delta_{t(CNT)}$.

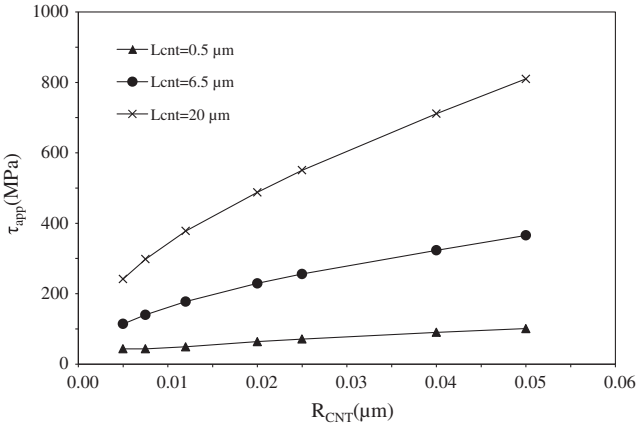

Fig. 7. Influence of CNT embedded length L_{CNT} and CNT radius R_{CNT} on the interfacial shear strength.

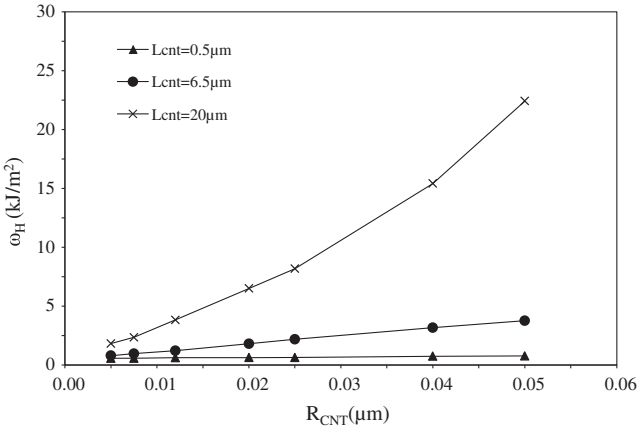

Fig. 8. Influence of CNT embedded length L_{CNT} and CNT radius R_{CNT} on the specific pullout energy.

3.3.2. CNT geometry effect

The effect of the CNT embedded length L_{CNT} and CNT radius R_{CNT} on the apparent interfacial shear strength τ_{app} is shown in Fig. 7. The CNT embedded length ranges from 0.5 to 20 μm and the CNT radius is selected from 0.005 to 0.05 μm [43]. It can be seen that the interfacial shear strength of the hybrid fibre increases with increases in both the CNT embedded length L_{CNT} and the CNT radius R_{CNT}. This is due to the increased CNT pullout force $F_{\max(CNT)}$ increases linearly with increases in both the CNT embedded length L_{CNT} and CNT radius R_{CNT} in the single CNT pullout. According to the definition of Eq. (3), the interfacial area of carbon fibre is kept as a constant, thus the apparent interfacial shear strength of hybrid fibre will increase with the increase of the CNT size or length.

The total pullout energy W_H consists of the debonding energy from carbon fibre pullout $W_{CF}(W_{CF} = 2G_{IIc(CF)}\pi R_{CF}L_{CF})$ and CNT pullout $W_{CNT}(W_{CNT} = 2G_{IIc(CNT)}\pi R_{CNT}L_{CNT})$ as $W_H = W_{CF} + W_{CNT}$. The specific pullout energy can be represented as

$$\omega_H = \frac{W_H}{2\pi R_{CF}L_{CF}} = G_{IIc(CF)} + \frac{G_{IIc(CNT)}R_{CNT}L_{CNT}}{R_{CF}L_{CF}} \quad (5)$$

where $G_{IIc(CF)}$ is fracture energy release rate from carbon fibre and $G_{IIc(CNT)}$ is fracture energy release rate from CNT pullout. According to Eq. (5), if the embedded length and radius of the carbon fibre does not be changed, the specific pullout energy of hybrid fibre ω_H should be increased by both the CNT embedded length and CNT radius. The numerical result showed in Fig. 8 confirms these analytical findings, which also indicates that increasing the size of CNTs can enhance the fibre bridging effect. Garcia et al. [39] and Wicks and Wardle [44] also reported an increase of toughness due to the increase of CNT length in their experiment study. In practice, the size and density of CNTs grown on the carbon fibre may be restrained during synthesis, while various size and density of CNTs can be simulated in this study. Additionally, CNTs may be fragmented or detached from the carbon fibre during the pullout in practice. CNT break occurs if the tensile stress is over its tensile strength and detachment occurs if the shear stress at the joint is over the shear strength. A longer CNT can contribute to both the increase of the tensile stress in CNT and the shear stress at the joint during a pullout of the hybrid fibre.

4. Conclusion

In this paper, a new numerical method was proposed to simulate the multiscale CNT/CF hybrid fibre pullout. Two finite element models were developed to simulate a single CNT pullout at microscale and to simulate the pullout of the hybrid fibre at macroscale. The bridging effect of the CNTs during the hybrid fibre pullout was represented by defining the properties of spring elements, which were obtained from a single CNT pullout simulation at microscale.

The numerical results of the CNT/CF hybrid fibre pullout from a case study show that growing CNTs on the carbon fibre has a significant effect on the maximum pullout force. The CNTs increase the resistance in the hybrid fibre pullout before the interfacial debonding occurs in carbon fibre. Consequently, there is a significant improvement in the interfacial shear strength. The increased specific pullout energy indicates that growing CNTs can enhance the fracture resistance of fibre reinforced composites. Applying the proposed numerical method for the CNT/CT hybrid fibre pullout, the effect of CNT–matrix interfacial bonding was investigated based on the main parameters involved in cohesive law used in the single CNT pullout. The numerical results show that the debonding force of CNT/CF hybrid fibre increases with increases in both interfacial crack initiation shear stress and CNT complete tangential separation displacement. In addition, the effect of the CNT geometry, represented by the CNT embedded length and the CNT radius, on the interfacial shear strength and the specific pullout energy was investigated. The numerical results show that the interfacial shear strength and the specific pullout energy of CNT/CF hybrid fibre significantly increases with increases in both CNT embedded lengths and CNT radii, which indicates that increasing the size or length of CNTs can enhance the hybrid fibre bridging effect.

References

[1] Beckman W. UC researchers shatter world records with length of carbon nanotube arrays; 2007. <http://www.uc.edu/News/NR.aspx?ID=5700> [cited 2012 06–11].
[2] Qian D, Dickey EC, Andrews R, Rantell T. Load transfer and deformation mechanisms in carbon nanotube–polystyrene composites. Appl Phys Lett 2000;76(20):2868–70.
[3] Chang TE, Jensen LR, Kisliuk A, Pipes RB, Pyrz RB, Sokolov AP. Microscopic mechanism of reinforcement in single-wall carbon nanotube/polypropylene nanocomposite. Polymer 2005;46(2):439–44.
[4] Thostenson ET, Li WZ, Wang DZ, Ren ZF, Chou TW. Carbon nanotube/carbon fiber hybrid multiscale composites. J Appl Phys 2002;91(9):6034–7.
[5] Bekyarova E, Thostenson ET, Yu A, Kim H, Gao J, Tang J, et al. Multiscale carbon nanotube–carbon fiber reinforcement for advanced epoxy composites. Langmuir 2007;23(7):3970–4.
[6] Sager RJ, Klein PJ, Lagoudas DC, Zhang Q, Liu J, Dai L, et al. Effect of carbon nanotubes on the interfacial shear strength of T650 carbon fiber in an epoxy matrix. Compos Sci Technol 2009;69(7–8):898–904.
[7] Zhang F-H, Wang R-G, He X-D, Wang C, Ren L-N. Interfacial shearing strength and reinforcing mechanisms of an epoxy composite reinforced using a carbon nanotube/carbon fiber hybrid. J Mater Sci 2009;44(13):3574–7.

[8] Godara A, Gorbatikh L, Kalinka G, Warrier A, Rochez O, Mezzo L, et al. Interfacial shear strength of a glass fiber/epoxy bonding in composites modified with carbon nanotubes. Compos Sci Technol 2010;70(9):1346–52.
[9] An F, Lu C, Li Y, Guo J, Lu X, Lu H, et al. Preparation and characterization of carbon nanotube–hybridized carbon fiber to reinforce epoxy composite. Mater Des 2012;33(1):197–202.
[10] Qian H, Bismarck A, Greenhalgh ES, Kalinka G, Shaffer MSP. Hierarchical composites reinforced with carbon nanotube grafted fibers: the potential assessed at the single fiber level. Chem Mater 2008;20(5):1862–9.
[11] Hung KH, Kuo WS, Ko TH, Tzeng SS, Yan CF. Processing and tensile characterization of composites composed of carbon nanotube–grown carbon fibers. Compos A Appl Sci Manuf 2009;40(8):1299–304.
[12] Pregler SK, Byeong-Woo J, Sinnott SB. Ar beam modification of nanotube based composites using molecular dynamics simulations. Compos Sci Technol 2008;68(9):2049–55.
[13] Liu YJ, Nishimura N, Qian D, Adachi N, Otani Y, Mokashi V. A boundary element method for the analysis of CNT/polymer composites with a cohesive interface model based on molecular dynamics. Eng Anal Bound Elem 2008;32(4):299–308.
[14] Namilae S, Chandra N. Multiscale model to study the effect of interfaces in carbon nanotube-based composites. J Eng Mater Technol Trans ASME 2005;127(2):222–32.
[15] Liao K, Li S. Interfacial characteristics of a carbon nanotube–polystyrene composite system. Appl Phys Lett 2001;79(25):4225–7.
[16] Kulkarni M, Carnahan D, Kulkarni K, Qian D, Abot JL. Elastic response of a carbon nanotube fiber reinforced polymeric composite: a numerical and experimental study. Compos B Eng 2010;41(5):414–21.
[17] Nie J, Jia Y, Qu P, Shi Q. Carbon nanotube/carbon fiber multiscale composite: influence of interfacial strength on mechanical properties. J Inorg Organomet Polym Mater 2011;21(4):937–40.
[18] Zheng Q, Xia D, Xue Q, Yan K, Gao X, Li Q. Computational analysis of effect of modification on the interfacial characteristics of a carbon nanotube–polyethylene composite system. Appl Surf Sci 2009;255(6):3534–43.
[19] Li L, Xia ZH, Curtin WA, Yang YQ. Molecular dynamics simulations of interfacial sliding in carbon-nanotube/diamond nanocomposites. J Am Ceram Soc 2009;92(10):2331–6.
[20] Fan CW, Liu YY, Hwu C. Finite element simulation for estimating the mechanical properties of multi-walled carbon nanotubes. Appl Phys A Mater Sci Process 2009;95(3):819–31.
[21] Fan C-W, Huang J-H, Hwu C, Liu Y-Y. Mechanical properties of single-walled carbon nanotubes – a finite element approach. Adv Mat Res 2008;33–37:937–42.
[22] Cooper CA, Cohen SR, Barber AH, Wagner HD. Detachment of nanotubes from a polymer matrix. Appl Phys Lett 2002;81(20):3873–5.
[23] ABAQUS. ABAQUS 6.11 documentation, Dassault Systèmes Simulia Corp.; 2012.
[24] Taljsten B. Strengthening of concrete prism using the plate-bonding technique. Int J Fract 1996;82(3):253–66.
[25] Teng JG, Yuan H, Chen JF. FRP-to-concrete interfaces between two adjacent cracks: theoretical model for debonding failure. Int J Solids Struct 2006;43(18–19):5750–78.
[26] Tsai JH, Patra A, Wetherhold R. Finite element simulation of shaped ductile fiber pullout using a mixed cohesive zone/friction interface model. Compos Part A (Appl Sci Manuf) 2005;36(6):827–38.
[27] Tvergaard V. Effect of fibre debonding in a whisker-reinforced metal. Mater Sci Eng A 1990;A125(2):203–13.
[28] Chaboche JL, Girard R, Levasseur P. On the interface debonding models. Int J Damage Mech 1997;6(3):220–57.
[29] Jia Y, Yan W, Liu H-Y. Carbon fibre pullout under the influence of residual thermal stresses in polymer matrix composites. Comput Mater Sci 2012;62:79–86.
[30] Yan W, Liu H-Y, Mai Y-W. Numerical study on the mode I delamination toughness of z-pinned laminates. Compos Sci Technol 2003;63(10):1481–93.
[31] Yan W, Liu H-Y, Mai Y-W. Mode II delamination toughness of z-pinned laminates. Compos Sci Technol 2004;64(13–14):1937–45.
[32] Li VC, Wang Y, Backer S. Effect of inclining angle, bundling, and surface treatment on synthetic fibre pull-out from a cement matrix. Composites 1990;21(2):132–40.
[33] Fu S-Y, Chen Z-K, Hong S, Han CC. The reduction of carbon nanotube (CNT) length during the manufacture of CNT/polymer composites and a method to simultaneously determine the resulting CNT and interfacial strengths. Carbon 2009;47(14):3192–200.
[34] Chen B, Yuan Q, Yun D-G, Fan J-H. Multiscale microstructure of chafer cuticle. Mater. Sci. Forum 2011;689:144–8.
[35] Lee Y, Kang S-T, Kim J-K. Pullout behavior of inclined steel fiber in an ultra-high strength cementitious matrix. Constr Build Mater 2010;24(10):2030–41.
[36] Zhang Q, Liu J, Sager R, Dai L, Baur J. Hierarchical composites of carbon nanotubes on carbon fiber: influence of growth condition on fiber tensile properties. Compos Sci Technol 2009;69(5):594–601.
[37] Daniel IM, Ishai O. Engineering mechanics of composite materials. 2nd ed. New York: Oxford University Press; 2006.
[38] Schaefer JD, Rodriguez AJ, Guzman ME, Lim C-S, Minaie B. Effects of electrophoretically deposited carbon nanofibers on the interface of single carbon fibers embedded in epoxy matrix. Carbon 2011;49(8):2750–9.
[39] Garcia EJ, Wardle BL, Hart AJ. Joining prepreg composite interfaces with aligned carbon nanotubes. Compos A Appl Sci Manuf 2008;39(6):1065–70.
[40] Yamamoto N, Hart AJ, Garcia EJ, Wicks SS, Duong HM, Slocum AH, et al. High-yield growth and morphology control of aligned carbon nanotubes on ceramic fibers for multifunctional enhancement of structural composites. Carbon 2009;47(3):551–60.
[41] Smiljanic O, Dellero T, Serventi A, Lebrun G, Stansfield BL, Dodelet JP, et al. Growth of carbon nanotubes on ohmically heated carbon paper. Chem Phys Lett 2001;342(5–6):503–9.
[42] Kim KJ, Kim J, Yu W-R, Youk JH, Lee J. Improved tensile strength of carbon fibers undergoing catalytic growth of carbon nanotubes on their surface. Carbon 2013;54:258–67.
[43] Baughman RH, Zakhidov AA, De Heer WA. Carbon nanotubes – the route toward applications. Science 2002;297(5582):787–92.
[44] Wicks SS, Wardle BL. Interlaminar fracture toughness of laminated woven composites reinforced with aligned nanoscale fibers: mechanisms at the macro, micro, and nano scales. Boston, MA, United states, April 8–11 AIAA 2013-1612; 2013.